THE AMERICAN SOCIETY OF MECHANICAL ENGINEERS
345 E. 47th St., New York, N.Y. 10017

97-GT-451

STUDIES ON WAKE-DISTURBED BOUNDARY LAYERS UNDER THE INFLUENCES OF FAVORABLE PRESSURE GRADIENT AND FREE-STREAM TURBULENCE PART I: EXPERIMETAL SETUP AND DISCUSSIONS ON TRANSITION MODEL

Ken-ichi Funazaki, Takashi Kitazawa and Kazuyuki Koizumi
Department of Mechanical Engineering
Iwate University
Morioka, Japan

Tadashi Tanuma
Heavy Apparatus Engineering Laboratory
Toshiba Corporation
Yokohama, Japan

ABSTRACT

The objective of this study is to investigate effects of favorable pressure gradient as well as free-stream turbulence upon wake-induced boundary layer transition on a flat plate. Likewise in the previous study by Funazaki (1996), a spoked-wheel type wake generator is employed in this study. Two identical flat plates with sharp edge are used as test model. One of them is for measurement of boundary layers over the test plate by use of a single hot-wire probe, and the other is provided with thin stainless-steel foils on the surface to measure wake-affected heat transfer along the surface. Free-stream turbulence intensities are controlled with several types of turbulence grids. Pressure gradients over the test surface are adjusted by changing an inclination angle of the plate located opposite to the test model. In Part I, transition models proposed by Mayle and Dullenkopf (1990b) and Funazaki (1996a, 1996b) are compared with the experimental data obtained in this study to examine how such a model succeeds or fails in predicting the wake-induced boundary layer transition under the influences of favorable pressure gradient with a low free-stream turbulence.

NOMENCLATURE

$b_{1/2}$	: semi-depth width of a bar wake
C_d	: drag coefficient of a circular cylinder
C_p	: specific heat
d	: diameter of wake generating bar
f	: bar-passing frequency ($=nn_c/60$)
L	: length of the test plate
L_e	: streamwise turbulence dissipation scale ($=(\overline{u'^2})^{3/2}/(Ud\overline{u'^2}/dx)$)
l_D	: distance from the locus of the wake generating bars and the leading edge of the test plate
n	: rotation number
n_c	: number of cylinders used
Pr	: Prandtl number
Re	: Reynolds number ($=U_\infty L/\nu$)
Re_θ	: momentum thickness Reynolds number
S	: Strouhal number ($=fL/U_\infty$)
St	: Stanton number
T_w, T_∞	: wall temperature, free-stream temperature
Tu	: turbulence intensity
$Tu_{\max}$	: peak value of the wake turbulence
Tu_∞	: inlet turbulence intensity
t	: time
U_∞	: inlet velocity
$U_e(x)$	: velocity at the outer edge of the boundary layer
u'	: streamwise velocity fluctuation
$\bar{v}(t_j)$	: ensemble-averaged velocity
$\tilde{v}_i(t_j)$	: sampled instantaneous velocity data
x	: streamwise distance from the leading edge
x_{tw}	: wake-induced transition onset
y	: distance from the test surface
β_E, β_F	: propagation speed ratios of the leading and trailing edges of wake-induced turbulent patch
$\gamma_w(x)$	: wake-induced intermittency
ρ	: density
ν	: kinematic viscosity
$\tau_{1/2}$	: semi-depth width of wake turbulence profile
τ_w	: wake duration
subscript	
L, T	: laminar, turbulent

INTRODUCTION

A number of studies have been devoted to the issues on wake-induced boundary layer transition (Pfeil and Herbst(1979), Addision and Hodson (1990a), (1990b), Mayle (1991), Schobeiri et al. (1994), Funazaki (1996a)). Recently, Halstead et al. (1995), using a low-speed research turbine and compressor, have provided systematic studies that give us a great insight into the physics of those complicated phenomena as well as excellent database to be compared with experimental or numerical analyses. Nevertheless, the present authors

Presented at the International Gas Turbine & Aeroengine Congress & Exhibition
Orlando, Florida — June 2–June 5, 1997

feel a great necessity for simple but well-controlled experiments in terms of pressure gradient as well as free-stream turbulence, since such experiments are still important to construct a design tool for estimation of wake-affected heat transfer around a turbine blade or additional profile loss of the cascade. Furthermore, they provide a detailed database that would be useful for modifying existing turbulence models so as to account for the wake-induced transitional behavior of the boundary layer.

Concerning the wake-induced boundary layer transition over the suction surface, the onset of the transition is likely to occur on a favorable pressure gradient region unless a separation bubble near the blade leading edge induces an earlier boundary layer transition. Blair (1992a, 1992b) or Reud and Witting (1984) made a comprehensive study on boundary layer transition in accelerating flows with various levels of free-stream turbulence intensity. Effects of the favorable pressure gradient on 'ordinary' boundary layer transition in turbomachines are well-documented by Mayle (1991). Keller and Wang (1996) executed detailed measurements of transitional boundary layers on a flat plate to investigate their flow and thermal behaviors under the streamwise flow acceleration. These studies have revealed that the thermal boundary layer experiences longer transition process than the momentum boundary layer in case of the favorable pressure gradient, thereby indicating inadequacy of Reynolds analogy for this case. Mayle also stated that the heat transfer data alone was not suitable for determining a streamwise intermittency distribution of the transitional boundary layer for non-zero pressure gradient cases, although the transition onset could be determined from the heat transfer data (Blair (1992b)).

Flow fields concerned become more complicated due to the effect of the periodic wake passage over the boundary layer because of the coexistence of a wake-induced transition and a natural (or 'ordinary') boundary layer transition. Orth (1992) measured the wake-disturbed unsteady boundary layer on a flat plate with the pressure gradient being controlled by changing its angle of attack against the inlet flow. Schobeiri and Radke (1994) examined the wake-induced boundary layer transition on the concave surface of a curved plate with zero or a favorable pressure gradient. In both studies a squirrel-cage type wake generator was used and no attempt was made to control the free-stream turbulence intensity.

Information on wake-affected heat transfer is available mostly from cascade tests or rotating rig tests and very few studies concerning the heat transfer on a flat plate have been made except for the study done by Funazaki (1996a). Blair et al. (1988a, 1988b) provided an extensive database on time-averaged heat transfer distributions over a rotor blade in the 1-1/2 turbine stage, some of which were compared with a correlation based on the intermittency factor by Sharma et al. (1988a). Dullenkopf et al. (1990) also measured time-averaged heat transfer around a turbine blade in the cascade subjected to periodic wakes from a spoked-wheel type wake generator. Utilizing these data or their preceding data given by Witting et al. (1988b), Mayle and Dullenkopf (1990b) developed their well-known theory for wake-induced transition. Zhang and Han (1995), using similar facilities to those of Dullenkopf et al. (1990), examined combined effects of free-stream turbulence and incoming wakes on heat transfer around a turbine blade. Zhang and Han found that it was necessary to make a upward shift of wake-induced transition onset with the increase in wake passing frequency (or wake Strouhal number) in order to achieve a reasonable agreement between the experiment and the theory of Mayle and Dullenkopf. They also mentioned that such an agreement became poor near the transition onset point for high Strouhal number cases since the flow acceleration reportedly suppressed the production of turbulence spots. This implies a possibility that the Mayle-Dullenkopf model is not well-implemented with any information on the effect of pressure gradient, although Mayle and Dullenkopf (1990a) showed that their model matched the data obtained at the experiments using not only a flat plate but also turbine cascades in which the flow acceleration around the blade surface surely affected the wake-induced transition.

The present study is divided into two parts. In Part I, the experimental setup is described at first, followed by the demonstration of the wake-affected heat transfer data obtained under the low free-stream turbulence condition. Discussions in Part I are limited to the wake-induced transition models proposed by Mayle and Dullenkopf (1990b) as well as by Funazaki (1996a, 1996b), which are compared with the experimental data. In Part II, detailed measurements of wake-affected heat transfer as well as unsteady boundary layer are conducted in order to clarify how a favorable pressure gradient affects the wake-induced transition of boundary layers on a flat plate under the controlled free-stream turbulence conditions.

TEST APPARATUS

Figure 1 presents the test apparatus used in this study, which is almost the same as that of the previous study done by Funazaki (1996a). Air from the blower, passing through the settling chamber and the contraction nozzle, entered the transition duct with less than 0.5% free-stream turbulence intensity. The test channel was inserted into the duct with a clearance between the channel and the duct to obtain uniform inflow into the test duct by discharging some amount of air from the clearance. Two types of the test plate were used in this study for the flow and the heat transfer measurement. Each of the test plate, which was of 1000 mm length and 10 mm thickness, was horizontally placed inside the test channel along the mid-height line of the duct. Since it had been anticipated that a separation bubble might occur at the leading edge of the test plate due to the flow asymmetry caused by the sharp-edged leading edge, a small fence was therefore equipped at the rear end of the test plate as a flow-controlling device to avoid this problem. Smooth inlet flow condition to the test plate was consequently achieved, which was confirmed by an oil-flow pattern and a tuft motion.

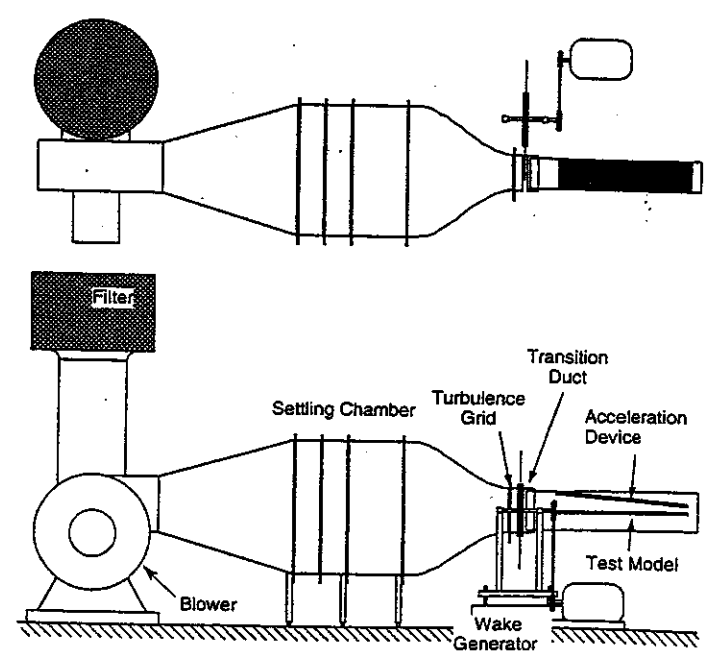

Figure 1 Test apparatus

Table 1 Configurations of turbulence grids

	Grid 1	Grid 2
Wire Diameter	0.8 mm	1.9 mm
Mesh Width	5.0 mm	10.0 mm
Inlet Turbulence Intensity Tu_∞	1.4 %	2.8 %
Dissipation Scale L_e	2.8 mm	4.2 mm

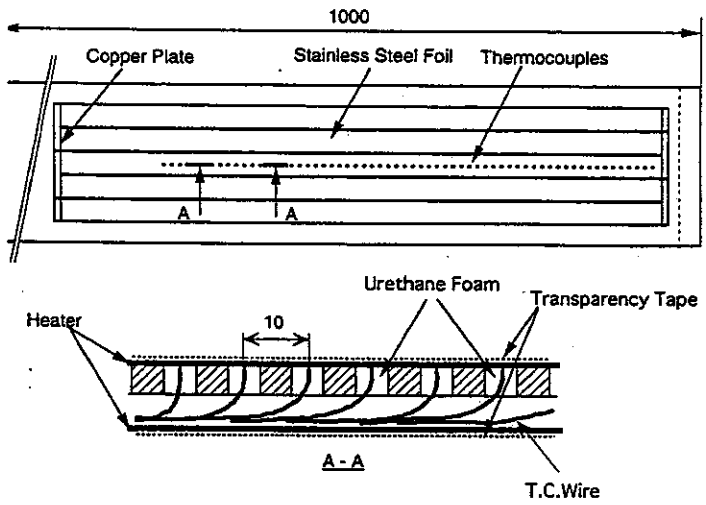

Figure 2 Test plate for heat transfer measurements

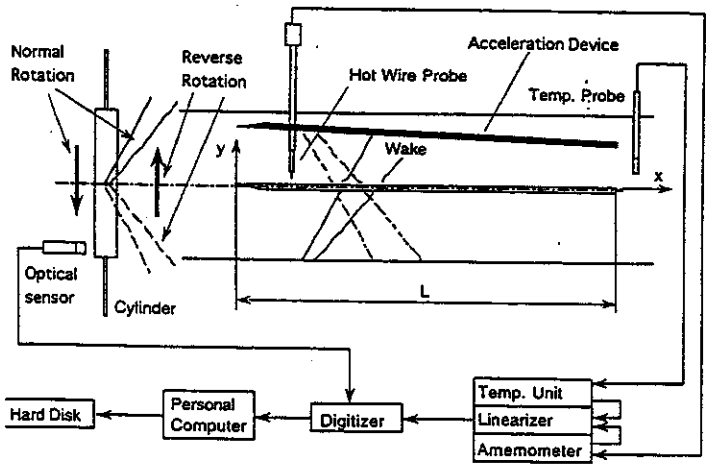

Figure 3 Setup for the flow measurement

The test plate for the flow measurement was implemented with several pressure taps situated near the plate center line in order to measure the pressure distribution over the test surface. Each of the pressure taps was connected to a high-precision Betz-type manometer with a tube. The test plate for the heat transfer measurement shown in Figure 2 was provided with K-type thermocouples. Hot junctions of the thermocouples were flush-mounted on the test surface along th center line of the plate, over which stainless-steel foil tapes of 30 μm thickness were covered as a heater to achieve a constant heat flu condition on the surface. To minimize the heat conduction loss throug the test plate, the back side of the test plate was also covered with th stainless-steel foil tapes in a quite similar manner to the test surfac All foils including those on the back side were connected with eac other via copper plates so as to form a in-line circuit. An electri power supplied to heat the foils were controlled by a power regulato

A spoked-wheel type wake generator was utilized to simulat periodic wakes passing over the boundary layer of the test model Cylindrical bars of 250 mm length and 5 mm diameter were attache to the disk rim of the wake generator. The streamwise distance betwee the locus of the bars and the plate leading edge (l_D) was 200 mm. A rotation speed n was controlled with the transmission gear box, being monitored with an optical tachometer. By changing the rotation directio of the wake generator it could produce two types of the wakes tha affected the boundary layer on the test surface in different manners, a shown in Figure 3. When the bars moved downward in front of th plate (designated as 'normal rotation' case), they generated wakes tha impinged the test surface. On the other hand, when the bars wen upwards ('reverse rotation' case), they produced wakes that exhibite 'sink-like' behavior on the test surface. One should remember that th wakes of the normal (or reverse) rotation case impacted the test surfac in a similar manner to wakes over the turbine (or compressor) suctio surface in real turbomachines. A great care was paid to the location o the wake generator relative to the test plate. The disk axis was situate at almost the same height with the plate surface from the ground, so that each of the bars became aligned with the leading edge of the tes plate when it moved in front of the plate. This arrangement made it possible to achieve nearly two-dimensional contact of the wakes with the boundary layer over the test plate.

Two types of turbulence grids were adopted to enhance the inle free-stream turbulence intensity. The grid configurations and the turbulence intensities generated are listed in Table 1. Each of the grids was attached to the exit of the contraction nozzle 300 mm distanced from the leading edge of the test plate. Note that the turbulence intensities appeared in Table 1 were measured nearby the leading edge of the plate ($x/L=0.05$, $y/d=2$). A streamwise pressure gradient was controlled by changing an inclination of the additional plate equipped at the upper portion of the test duct. This plate was provided with a slit through which a hot-wire probe penetrated the flow, any leakage from the slit being carefully avoided. As for the decay rate of the free-stream turbulence over the measurement section, it was found that the free-stream turbulence reduced approximately by a factor of two with the presence of the favorable pressure gradient, while it substantially remained constant in the no flow-acceleration case.

Instruments and Data Processing

Figure 3 shows the system for the boundary layer measurement. An I-type hot-wire probe was traversed in the direction normal to the plate surface at several streamwise locations to obtain instantaneous velocity profiles of the boundary layer. The data processing system consisted of a CTA with a linearizer (Kanomax, System 7201), an A/D convertor (Autonix, APC-204) and a PC for controlling the system. Data sampling frequency was 50 kHz. Each of the data-acquisition processes was triggered with a signal from the optical tachometer, which made test data synchronized with the disk revolution. These digitized velocity data for each traversing location, $u_i(y,t_j)$, were then used to calculate an ensemble-averaged velocity $\bar{u}_i(y,t_j)$ and a local turbulence intensity $Tu(t_j)$ as follows;

$$\tilde{u}(y,t_j)=\frac{1}{k}\sum_{i=1}^{k}u_i(y,t_j)\ ,\ j=1,...,2048\ ,\ k=256\ , \qquad (1)$$

$$Tu(t_j)=\sqrt{\frac{1}{k-1}\sum_{i=1}^{k}\left[u_i(t_j)-\tilde{u}(t_j)\right]^2}\ \Big/ U_e(x)\ , \qquad (2)$$

where $U_e(x)$ represents the velocity at the outer edge of the boundary layer, which was determined from the Bernoulli's theorem using measured pressure distribution along the plate. Inlet velocity U_∞ was measured by a standard Pitot tube.

Signals of the thermocouples were acquired by a PC-control datalogger. The data acquisition was invoked after confirming their equilibrium state of the temperature distribution. Stanton number is then obtained as follows;

$$St(x)=\frac{\dot{q}_{supply}-\dot{q}_{loss}}{C_p U_e(x)\left(T_w(x)-T_\infty\right)}\ , \qquad (3)$$

where q_{supply} is the heat flux determined from the power supplied to the heater on the plate surface, and q_{loss} represents heat loss due to heat conduction, heat radiation and somewhat parasitic heat generation at the copper plates. The temperature difference $T_w(x)-T_\infty$ was kept to be 10~15 °C through the test run. A preliminary test and an analytical estimation provided a correlation for evaluating the heat loss.

Uncertainty Analysis

Precision of pressure measurement using the Betz-type manometer was about ±1 [Pa], which resulted in about 0.4 % uncertainty of the static pressure measured on the test plate. Uncertainties of the inlet velocity and instantaneous velocity measurements were about 2 % and 3 %. The temperature measurement was of ±0.25 [°C] precision and the wall heat flux contains 2 % uncertainty. Therefore the uncertainty of the Stanton number was about 8 %.

RESULTS

Flow Condition

Inlet flow velocity U_∞ was almost 20 m/s for all test cases and the Reynolds number based on U_∞ and the plate length L (=1 m) was 1.3×10^6. Inlet free-stream turbulence intensity was about 0.5 %. Wake-disturbed flow field was characterized by the wake-passing Strouhal number S defined as follows;

$$S=fL/U_\infty\ ,\quad f=nn_c/60\ , \qquad (4)$$

where the number of the cylinders n_c varied from 2 to 6 with the rotation speed n being fixed at 1130 rpm. A flow acceleration level is indexed in terms of the acceleration parameter K, defined as

$$K=\frac{\nu}{U_e^2}\frac{dU_e}{dx}\ . \qquad (5)$$

Velocity Distributions

In the present study four inclination angles of the flow accelerating device were adopted. Figure 4 shows the velocity distributions measured for these cases and the resultant acceleration parameters averaged over the region from the leading edge to x/L=0.6 are listed in Table 2. Note that due to a mechanical restriction, for higher acceleration cases designated as type 3 and type 4 the flow accelerated until x/L =0.6, followed by a deceleration.

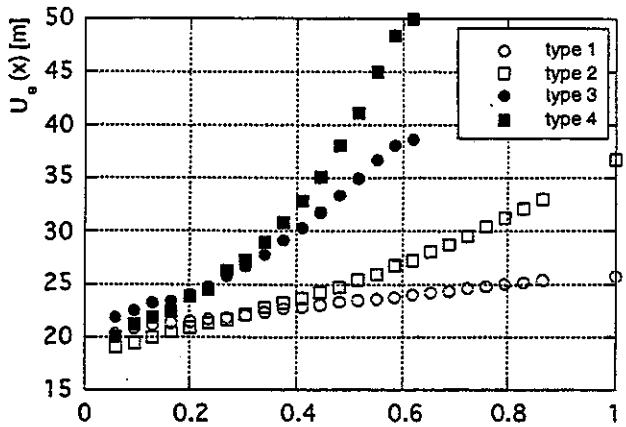

Figure 4 Velocity distributions along the plate

Table 2 Acceleration parameter

	type 1	type 2	type 3	type 4
$K\times10^6$	0.2	0.4	0.55	0.75

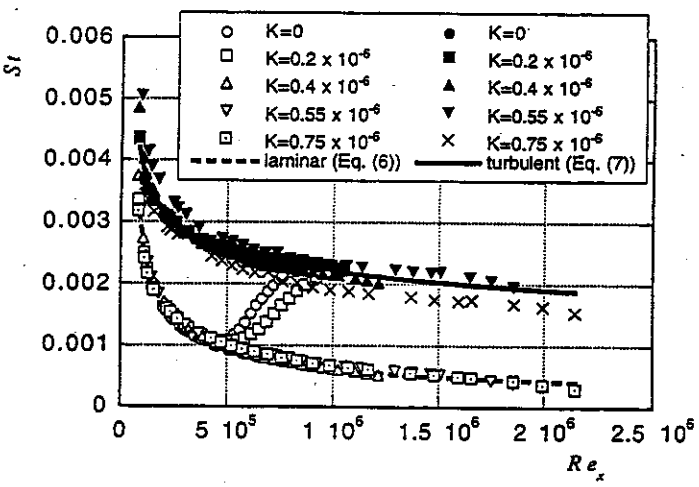

Figure 5 Stanton number distributions for the cases of no wake and low free-stream turbulence

Heat Transfer

Figure 5 shows the Stanton number distributions for the cases of no wake and low free-stream turbulence. Also shown are correlations for a laminar and a turbulent boundary layers over the surface with constant heat flux for comparison, which are given as follows (Keller and Wang, 1996):

$$St=0.453Pr^{-2/3}Re_x^{-1/2}\left[1-\left(x_0/x\right)^{3/4}\right]^{-1/3}\ , \qquad (6)$$

$$St=0.03Pr^{-0.4}Re_x^{-0.2}\left[1-\left(x_0/x\right)^{0.9}\right]^{-1/9}\ , \qquad (7)$$

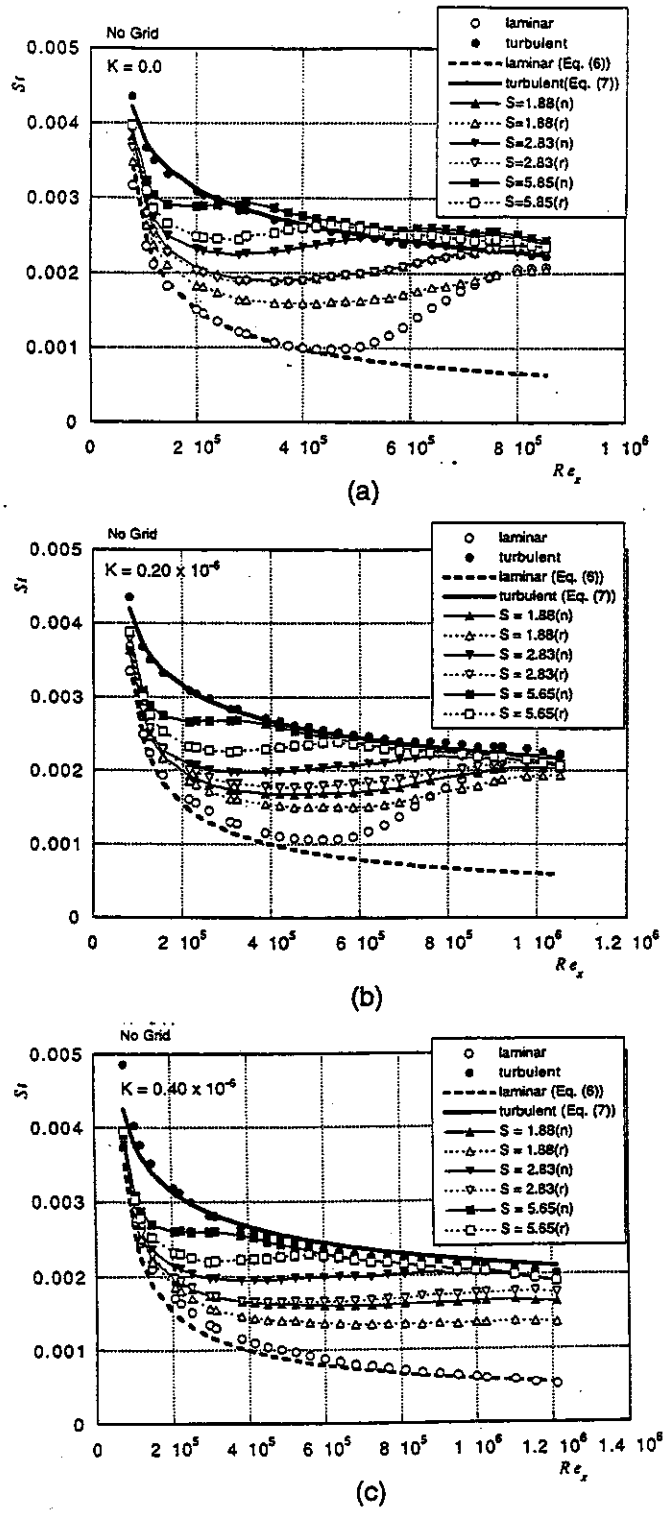

Figure 6 Stanton number distributions for the cases of no wake and low free-stream turbulence
(a) $K=0.0$ **(b)** $K=0.20\times10^{-6}$ **(c)** $K=0.40\times10^{-6}$

where x_0 is the unheated starting length and 45 mm for the present case. Fully turbulent states of the boundary layer, which are represented by solid symbols in Figure 5, were achieved by use of a circular cylinder that was situated in front of the test plate perpendicularly to the leading edge of the test plate. It is evident from Figure 5 that the measured heat transfer data match the correlations fairly well, which demonstrates the soundness of the present experiment. This figure also shows that the natural transition was suppressed by the flow acceleration of $K \geq 0.4\times10^{-6}$.

Figure 6 shows wake-affected Stanton number distributions for three flow acceleration parameters. Note that this figure contains the data not only for the normal rotation cases but also for the reverse rotation cases in order to demonstrate how the difference in motion of the wake-generating bar relative to the test plate affects the wake-induced transition process. It is clear that the heat transfer over the test plate was enhanced due to the wake passage and such a tendency became pronounced with the increase in wake passing frequency or Strouhal number. Readers might notice a distinct difference between the heat transfer enhancements caused by 'normal rotation' and 'reverse rotation' wakes. Most plausible explanation on this difference is a negative jet effect of the wake. A relevant discussion on this matter will be given in the following.

Intermittency Factor

Definition. In order to examine effects of favorable pressure gradient on wake-induced boundary layer transition, an intermittency factor $\gamma_w(x)$ is calculated, which is defined as

$$\gamma_w(x)=\frac{St(x)-St_L(x)}{St_T(x)-St_L(x)}, \tag{8}$$

where $St(x)$, $St_L(x)$ and $St_T(x)$ are wake-affected, laminar and turbulent Stanton number distributions, respectively. As mentioned earlier, the heat-transfer-based intermittency factor $\gamma_w(x)$ is not always the same as an intermittency factor determined from boundary layer measurements. Nevertheless, $\gamma_w(x)$ could be useful information to understand how and to what extent a flow acceleration influences the transition process including the transition onset. Comparisons are made between the experiment and a transition model such as

$$\gamma_w(w)=1-\exp\left(-1.9S\left(\frac{x-x_{tw}}{L}\right)\right), \tag{9}$$

proposed by Mayle and Dullenkopf (1990b), or

$$\gamma_w(x)=\min\left[1,\Gamma(x)\right], \tag{10}$$

$$\Gamma(x)=S\left(\frac{1}{\beta_E}-\frac{1}{\beta_F}\right)\int_{x_{tw}/L}^{x/L}\frac{U_\infty}{U(x')}dx'+\frac{\tau_w}{\tau}, \quad x\geq x_{tw}$$
$$=\frac{\tau_w}{\tau}, \quad x<x_{tw} \tag{11}$$

proposed by Hodson (1989), Hodson et al. (1992) and Funazaki (1996a). Wake duration τ_w, defined as a time length for which more than 4 % turbulence intensity lasts within the wake, can be calculated from the following correlation that is derived on a basis of a wake turbulence profile viewed from the stationary frame of reference.

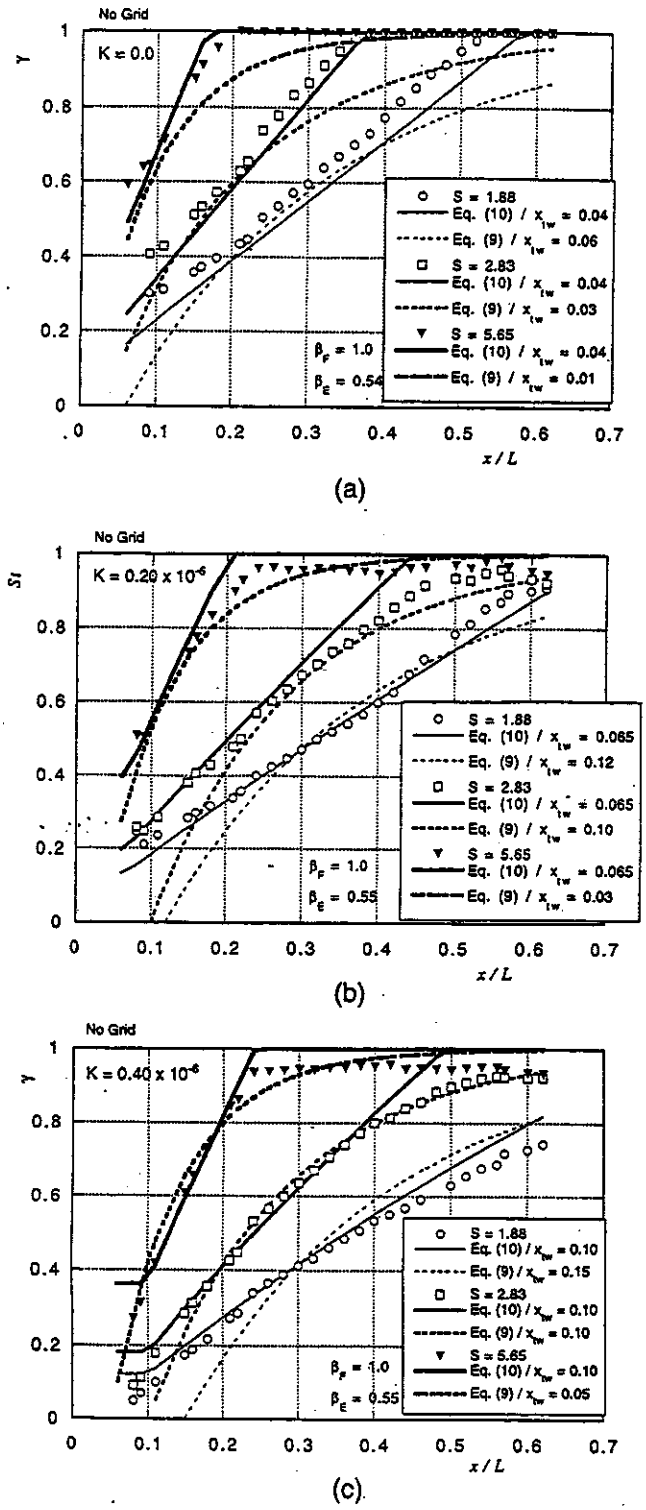

Figure 7. Intermittency factor distributions for the cases of no wake and low free-stream turbulence (normal rotation)
(a) $K=0.0$ **(b)** $K=0.20\times10^{-6}$ **(c)** $K=0.40\times10^{-6}$

$$\tau_w = 3.36\tau_{1/2}\sqrt{-\ln\left(4/Tu_{\max}\right)},\quad \tau_{1/2} \cong \frac{1.5b_{1/2}}{U_m\cos\lambda_w},\qquad (12)$$

$$b_{1/2} = 0.308\sqrt{C_d d\left(x+l_D\right)/\cos\lambda_w}\ ,\quad \lambda_w = \tan^{-1}\left(\frac{U_m}{U_\infty}\right)$$

where U_m is a moving speed of the wake-generating bar.

Normal Rotation Case. Figure 7 shows the intermittency factors determined from Eq. (8) for the normal rotation case, in conjunction with the results calculated by Eqs. (9) and (10). Uncertainty of the estimated intermittency factor is about 16%. As for the propagation speed ratios of wake-induced turbulent patch, $\beta_F=1$ and $\beta_E=0.55$ are adopted as suggested by Funazaki (1996a). The transition onset location x_{tw} is determined so as to obtain the best agreement with the corresponding experimental data for both models. Note that x_{tw} is assumed to be independent of the Strouhal number for the Funazaki model.

For K = 0.0, the wake-induced intermittency factors linearly vary with x/L and they almost follow the results given by Eq. (10), while Eq. (9) doesn't seem to yield any satisfactory results. Wake-induced transition onset is invoked at x_{tw}/C=0.03 ($Re_\theta \cong 140$) in case of using the Funazaki model. For $K=0.20\times10^{-6}$ and $K=0.40\times10^{-6}$, Eq. (10) still produces good agreements with the experiments, where x_{tw}/C=0.065 ($Re_\theta \cong 200$) and x_{tw}/C=0.10 ($Re_\theta \cong 240$), respectively. Eq. (9) also yields fairly good estimations at the second half of the transition process. However, Eq. (9) tends to underestimate the wake-induced intermittency factor near the start of the transition. Similar findings were reported by Han et al. (1993) in the experiment using a turbine blade cascade.

Reverse Rotation Case. As seen in Figure 6, reverse rotation of the wake generator yielded lower wake-affected heat transfer compared to the heat transfer obtained at the normal rotation. It is evident that the transition model of Eq. (10) cannot predict this phenomenon as it is unless a downward shift of the transition onset or any changes in the propagation speed ratios of wake-induced turbulence patch is implemented in the model. As shown in the last section of this paper, observations by means of a hot-wire probe located close to the plate surface revealed that wake duration for the reverse rotation tended to be shortened in comparison with that of the normal rotation, probably due to a negative jet effect, and that the leading edge of wake-induced turbulent patches moved at about 90% speed of the free-stream. Taking account of these findings, wake-affected intermittency factors for the reverse rotation case are calculated and are compared with the experimental data as shown in Figure 8. In this case β_F is reduced from 1.0 to 0.88, while β_E is unchanged and x_{tw} is the same as that of the corresponding normal rotation case. Furthermore, halved values of the wake durations given by Eq. (12), in conjunction with the original values for comparison, are adopted. Figure 8 reveals that the transition model with $\beta_F=0.88$ and the halved wake duration yields a fairly good agreement with the experiment for all cases, compared with the results for $\beta_F=0.88$ and the original wake duration (Eq. (12)). Recalling that the value 0.88 coincides with the propagation speed ratio of a turbulent spot given by Schubauer and Klebanoff (1958), it could be imagined that the effect of the turbulent spots becomes dominant in the transition process (or in the heat transfer enhancement) as the wake effect gradually diminishes due to the 'sink-like' behavior of the wakes generated in the reverse rotation case. Consequently, it seems natural to think that wakes produced in the

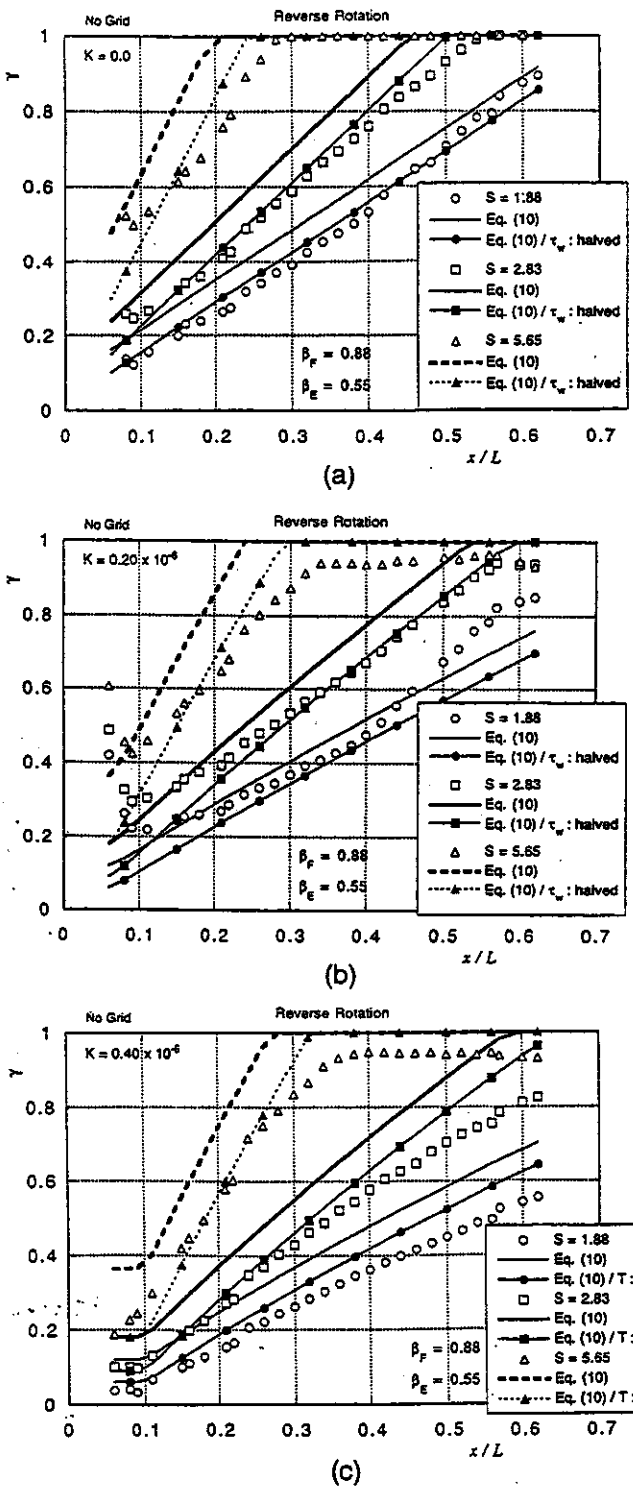

Figure 8 Intermittency factor distributions for the cases of no wake and low free-stream turbulence (reverse rotation)
(a) $K=0.0$ **(b)** $K=0.20\times10^{-6}$ **(c)** $K=0.40\times10^{-6}$

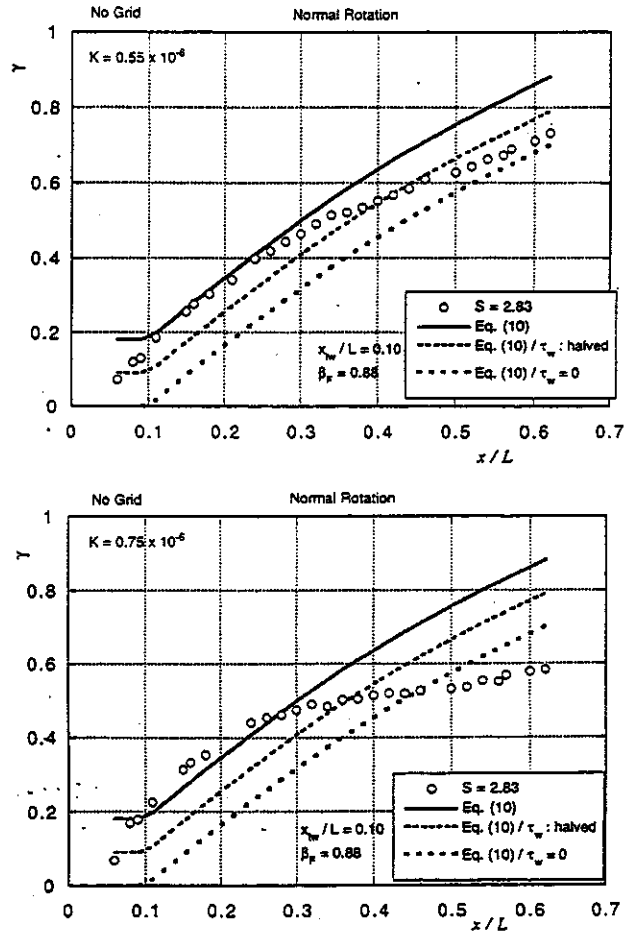

Figure 9 Intermittency factor distributions for higher flow acceleration cases (normal rotation)
(upper) $K=0.55\times10^{-6}$ **(lower)** $K=0.75\times10^{-6}$

normal rotation case are likely to compile on the test surface due to their 'jet-like' motion as the wakes moved along with the free-stream, pouring turbulence energy into the boundary layer.

High Flow Acceleration Case. Figure 9 shows the wake-affected intermittency factors for the flow acceleration of $K=0.55\times10^{-6}$ and $K=0.75\times10^{-6}$. Calculated results are also shown for three wake durations, say, the original value from Eq. (10), its halved value and zero, where x_{tw}/L=0.10 ($Re_\theta \cong 260$) . This figure clearly shows that such a high flow acceleration significantly affected the wake-induced transition process so that the growth rate of the intermittency factor tended to be slowed compared to the estimated one, however the experimental data matched the estimation at the early stage of the transition, implying that it took some moment for the flow acceleration to be active to the transition. As pointed out by several researchers, a thermal boundary layer experiences longer transition process than the momentum boundary layer in case of favorable pressure gradient, which seemingly explains the situation of the present case to some extent. In addition, it appears that the wake itself was affected by such an intense flow acceleration so that its turbulence intensity suffered from considerable decay as the wake was convected downward, which

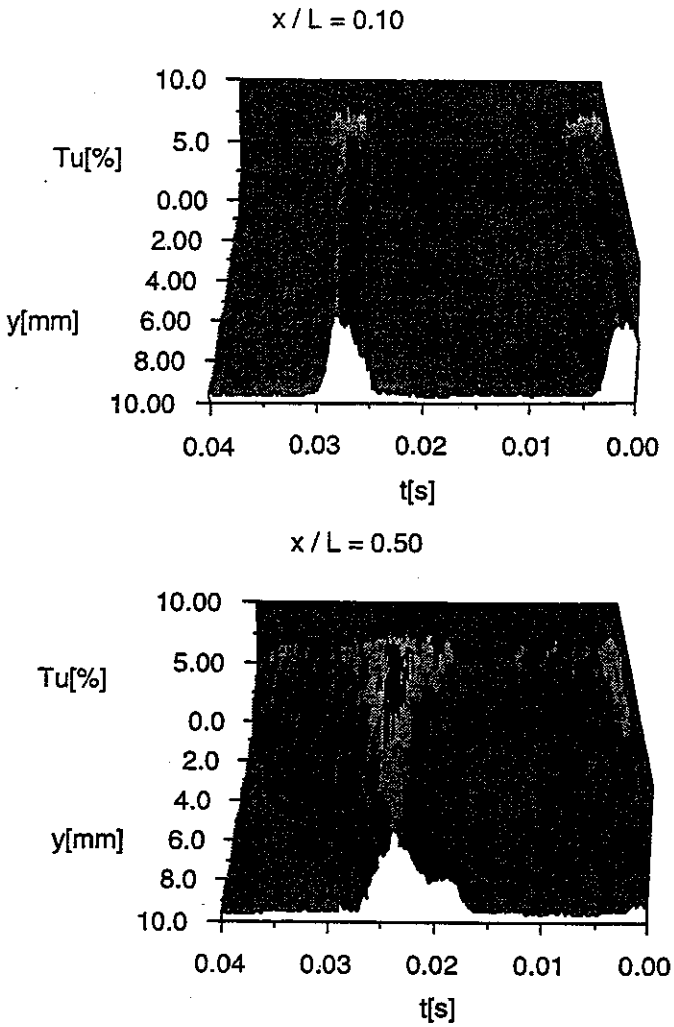

Figure 10 Perspective presentations of ensemble-averaged turbulence intensity for S=1.88 (normal rotation)

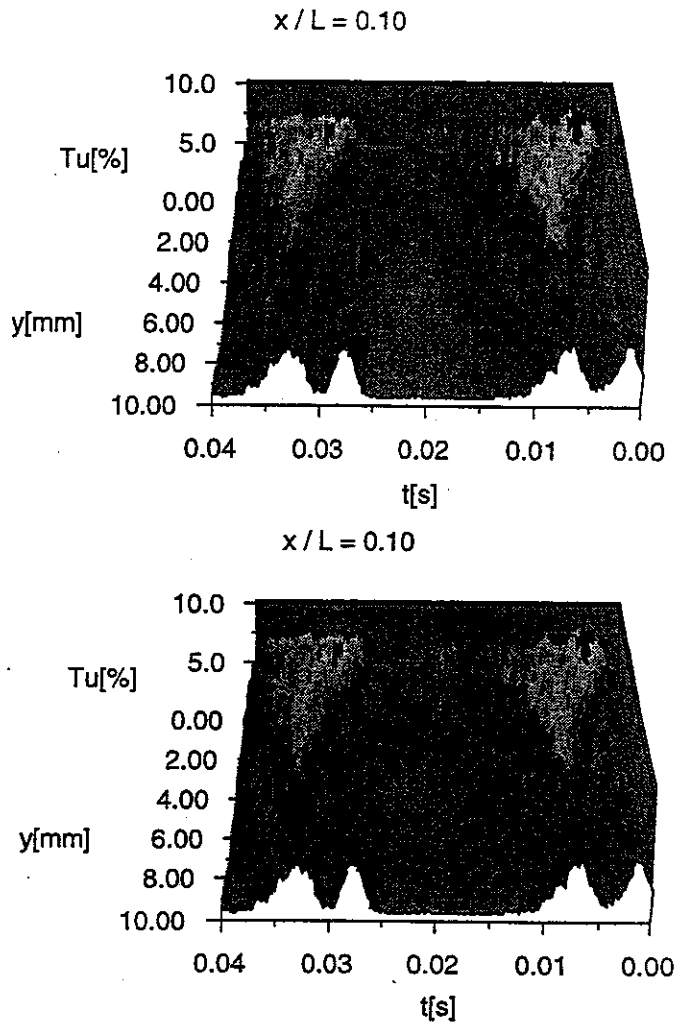

Figure 11 Perspective presentations of ensemble-averaged turbulence intensity for S=1.88 (reverse rotation)

could be another cause for the delayed transition as seen above.

Propagation Speed of the Turbulence Patch

Observations of wake-disturbed boundary layers by use of a hot-wire probe were made to determine the propagation speed of the turbulence patch induced by the wake passage. Figures 10 and 11 are perspective presentations of the ensemble-averaged turbulence intensity measured at x/L=0.10 and x/L=0.50 for the normal and reverse rotation cases with no pressure gradient (S=1.88). Figure 10 shows that the wake turbulence and the subsequent turbulence cluster (wake-induced turbulence patch) remain being mixed with each other until the merger of two neighboring turbulence clusters occurs. This implies that the leading edge of the turbulence patch moved at the free-stream speed, as expected in the transition model. On the other hand, Figure 11 demonstrates that a wake-induced turbulence patch for the reverse rotation case tended to lag behind the wake turbulence, resulting in a separation between the wake turbulence and the turbulence cluster.

This situation is confirmed by comparing several traces of ensemble-averaged turbulence intensity measured at y/L=0.0002 with those at y/L=0.01, as shown in Figure 12. Peaks of the traces for y/L=0.01 designated with P_1, which corresponded to the wake turbulence, moved almost at a speed of the free-stream, the peak value being decreasing. Meanwhile, peaks of the traces for y/L=0.0002 designated with P_2 moved almost at 90% free-stream speed. It is accordingly evident that the peaks P_2 were associated with wake-induced turbulence spots. One might notice an occurrence of another peak following the peak P_2 for x/L=0.50, which was actually a top of the growing wake-induced turbulence spots detected at y/L=0.01. Again this indicates separation between the wake turbulence and the associated turbulence spots occurred for the reverse rotation case. Walker (1993) found in his experiment using an axial compressor that the turbulence patch in the boundary layer on the suction surface of the compressor blade occurred at the end of the wake passage and did not coincide with the peak turbulence inside the wake. The present authors believe that the above-mentioned separation has a close relationship with Walker's

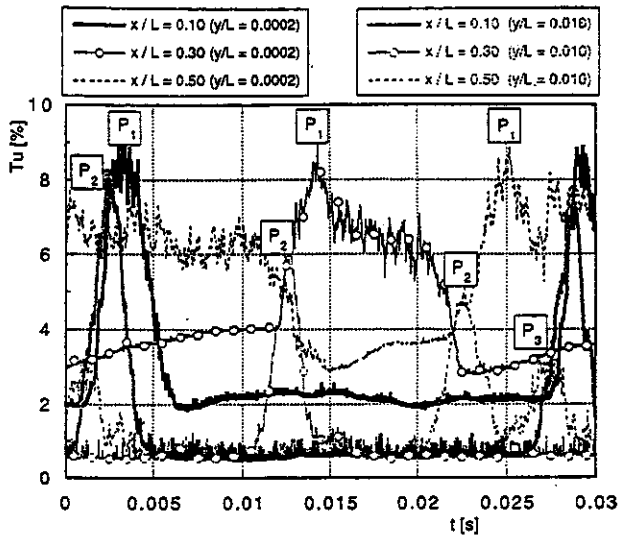

Figure 12 Traces of wake-affected turbulence intensity measured at three streamwise locations for reverse rotation case (S=1.88)

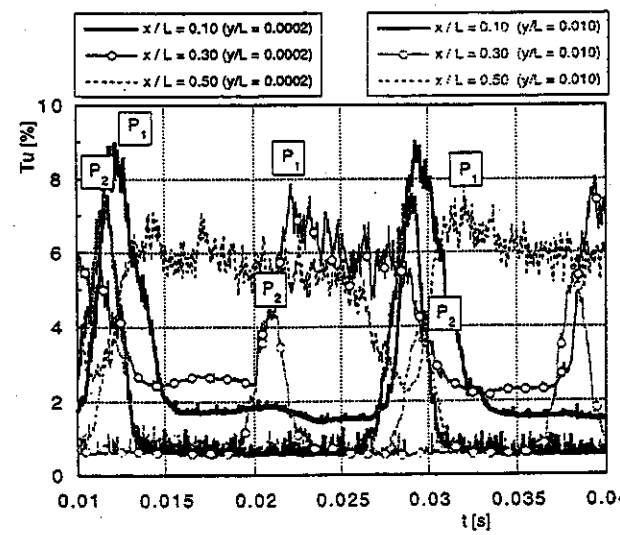

Figure 13 Traces of wake-affected turbulence intensity measured at three streamwise locations for reverse rotation case (S=1.88) with a favorable pressure gradient ($K = 0.40 \times 10^{-6}$)

observation. Figure 13 also represents several traces of ensemble-averaged turbulence intensity obtained at the same positions as in Figure 12 under a favorable pressure gradient ($K = 0.40 \times 10^{-6}$). Note that the definition for the turbulence intensity uses a local velocity $U_e(x)$ as denominator. From this figure with some calculations it follows that the peak P_1 moved at 90% speed of the free-stream on average, while the peak P_2 moved along with the free-stream. A comparison between Figures 12 and 13 shows that the peak P_3 observed in Figure 12 cannot be identified in Figure 13. This means that wake-induced turbulence spots under the flow acceleration grew slowly compared to that of no flow acceleration.

CONCLUSIONS

This paper, as Part I of our study, described the experimental setup, then demonstrated the experimental data of wake-affected heat transfer distributions over the test plate under the low free-stream turbulence condition. Also were made some discussions on the capability of two models proposed by Mayle and Dullenkopf (1990b) and Funazaki (1996a) for predicting intermittent behavior of wake-disturbed boundary layer under a favorable pressure gradient. The findings in the paper were summarized as follows:

(1) For moderate flow acceleration cases, wake-induced intermittency factors increased almost linearly with the surface length from the transition onset. Funazaki model successfully reproduced such a behavior of the boundary layer. Mayle-Dullenkopf model also exhibited a fairly good performance in predicting the intermittency factor, however, it failed to yield a satisfactory result at the early stage of the wake-induced transition.

(2) It was found that the reverse rotation of the wake-generator resulted in slower growth rate of the intermittency factor towards the downstream compared to the normal rotation case. Such a tendency could be well reproduced by Funazaki model in which β_F was changed from 1.0 to 0.88 and original value of τ_w was reduced by a factor of two. This implies that a 'sink-like' behavior of the wake on the test surface weakened the wake turbulence near the surface and wake-induced turbulent patches accordingly dominated the intermittent behavior of the boundary layer.

(3) High flow acceleration significantly affected the wake-induced transition process so that the growth rate of the intermittency factor tended to delay compared to the estimation. Nevertheless, the estimation matched the experimental data at the early stage of the transition.

(4) Locations of wake-induced transition onset were found around at $Re_\theta \equiv 200 \sim 250$ for favorable pressure gradient cases.

(5) Hot-wire measurements identified a separation between the wake turbulence and the wake-induced turbulence spots for the reverse rotation case, which was in contrast with the normal rotation case where they moved along with each other until the completion of the transition.

ACKNOWLEDGMENT

This program was partially funded by Komiya scholarship of Turbomachinery Society of Japan in 1995.

REFERENCES

Addison, J. S. and Hodson, H. P., 1990a, "Unsteady Transition in an Axial-Flow Turbine: Part I - Measurements on the Turbine Rotor," Trans.ASME *Journal of Turbomachinery*, Vol. 112, pp. 206-214.

Addison, J. S. and Hodson, H. P., 1990b, "Unsteady Transition in an Axial-Flow Turbine: Part II - Cascade Measurements and Modeling," Trans.ASME *Journal of Turbomachinery*, Vol. 112, pp. 215-222.

Blair, M. F., 1992a, "Boundary-Layer Transition in Accelerating Flow with Intense Freestream Turbulence: Part 1-Disturbances Upstream of Transition Onset," Trans. ASME *Journal of Fluids Engineering*, Vol. 114, pp. 313-321.

Blair, M. F., 1992b, "Boundary-Layer Transition in Accelerating Flow with Intense Freestream Turbulence: Part 2-The Zone of

INtermittent Turbulence," Trans. ASME *Journal of Fluids Engineering*, Vol. 114, pp. 322-331.

Blair, M. F., Dring, R. P. and Joslyn, H. D., 1988a, "The Effects of Turbulence and Stator/Rotor Interactions on Turbine Heat Transfer-Part I: Design Operating Conditions," ASME Paper 88-GT-125.

Blair, M. F., Dring, R. P. and Joslyn, H. D., 1988b, "The Effects of Turbulence and Stator/Rotor Interactions on Turbine Heat Transfer-Part II: Effects of Reynolds Number and Incidence," ASME Paper 88-GT-5.

Dullenkopf, K., Schulz, A. and Witting, S., 1990, "The Effect of Incident Wake Conditions on the Mean heat Transfer of an Airfoil," ASME Paper 90-GT-121.

Funazaki, K., 1996a, "Unsteady Boundary Layers on a Flat Plate Disturbed by Periodic Wakes: Part I - Measurement of Wake-Affected Heat Transfer and Wake-Induced Transition Model," Trans. ASME *Journal of Turbomachinery*, Vol. 118, pp. 327-336.

Funazaki, K., 1996b, "Unsteady Boundary Layers on a Flat Plate Disturbed by Periodic Wakes: Part II - Measurement of Unsteady Boundary Layers and Discussion," Trans. ASME *Journal of Turbomachinery*, Vol. 118, pp. 337-346.

Halstead, D. E., Wisler, D. C., Okiishi, T. H., Walker, G. J., Hodson, H. P. and Shin, H. W., 1995, "Boundary Layer Development in Axial Compressor and Turbines, Part 4 of 4: Computations and Analysis," ASME Paper 95-GT-464.

Han, J. C., Zhang, L. and Ou, S., 1993, "Influence of Unsteady Wake on Heat Transfer Coefficient From a Gas Turbine Blade," Trans. ASME *Journal of Heat Transfer*, Vol. 115, pp. 904 - 911.

Hodson, H. P., 1989, "Modelling Transition and Its Effects on Profile Loss," AGARD Conf. on Unsteady Flows in Turbomachines, AGARD CP 468.

Hodson, H. P., Addison, J. S. and Shepherdson, C. A., 1992, "Models for Unsteady Wake-Induced Transition in Axial Turbomachines," Journal de Physique III, Vol. 2, pp. pp. 545 - 574.

Keller, F. J. and Wang, T., 1996, "Flow and Heat Transfer Behavior in Transitional Boundary Layers with Streamwise Acceleration," Trans. ASME *Journal of Turbomachinery*, Vol. 118, pp. 314-326.

Mayle, R. E., 1991, "The Role of Laminar-Turbulent Transition in Gas Turbine Engines," Trans. ASME *Journal of Turbomachinery*, Vol. 113, pp. 509-537.

Mayle, R. E. and Dullenkopf, K., 1990a, "More on the Turbulent-Strip Theory for Wake-Induced Transition," ASME Paper 90-GT-137.

Mayle, R. E. and Dullenkopf, K., 1990b, "A Theory for Wake-Induced Transition," Trans. ASME *Journal of Turbomachinery*, Vol. 112, pp. 188-195.

Orth, U., 1992, "Unsteady Boundary-Layer Transition in Flow Periodically Disturbed by Wakes," ASME Paper 92-GT-283.

Pfeil, H. and Herbst, R., 1979, "Transition Procedure of Instationary Boundary Layer," ASME Paper 79-GT-128.

Rued, K. and Witting, S., 1984, "Free-Stream Turbulence and Pressure Gradient Effects on Heat Transfer and Boundary Layer Develeopment on Highly Cooled Surfaces," ASME Paper 84-GT-180.

Schubauer, G. B. and Klebanoff, P. S., 1958, "Contributions on the Mechanics of Transition," NACA TN 3489, NACA

Schobeiri, M. T. and Radke, R. E., 1994, "Effects of Periodic Unsteady Wake Flow and Pressure Gradient on Boundary Layer Transition along the Concave Surface of a Curved Plate," ASME Paper 94-GT-327.

Sharma, O. P., Renaud, E., Butler, T. L., Milsaps, J., K., Dring, R. P. and Joslyn, H. D., 1988a, "Rotor-Stator Interaction in Muti-Stage Axial-Flow Turbines," 24th AIAA/ASME/SAE/ASEE Joint Propulsion Conference.

Walker, G. J., 1993, "The Role of Laminar-Turbulent Transition in Gas Turbine Engines:A Discussion," Trans. ASME *Journal of Turbomachinery*, Vol. 115, pp. 207-217.

Witting, S., Schulz, A., Dullenkopf, K. and Fairbank, J., 1988b, "Effects of Free-Stream Turbulence and Wake Characteristics on the Heat Transfer Along a Cooled Gas Turbine Blade," ASME Paper 88-GT-179.

Zhang, L. and Han, J. C., 1995, "Combined Effect of Free-Stream Turbulence and Unsteady Waske on Heat Transfer Coefficients from a Gas Turbine Blade," Trans. ASME *Journal of Heat Transfer*, Vol. 117, pp. 296-302.